A βPix–Pak2a signaling pathway regulates cerebral vascular stability in zebrafish

Jing Liu*, Sherri D. Fraser*, Patrick W. Faloon†, Evvi Lynn Rollins*, Johannes Vom Berg*, Olivera Starovic-Subota*, Angie L. Laliberte*, Jau-Nian Chen‡, Fabrizio C. Serluca†, and Sarah J. Childs*§

*Department of Biochemistry and Molecular Biology, University of Calgary, 3330 Hospital Drive NW, Calgary, AB, Canada T2N 4N1; ‡Department of Molecular, Cellular, and Developmental Biology, University of California, Los Angeles, CA 90095; and †Novartis Institutes for BioMedical Research, 250 Massachusetts Avenue, Cambridge, MA 02139

Edited by Eric N. Olson, University of Texas Southwestern Medical Center, Dallas, TX, and approved May 8, 2007 (received for review February 3, 2007)

The vasculature tailors to the needs of different tissues and organs. Molecular, structural, and functional specializations are observed in different vascular beds, but few genetic models give insight into how these differences arise. We identify a unique cerebrovascular mutation in the zebrafish affecting the integrity of blood vessels supplying the brain. The zebrafish *bubblehead* (*bbh*) mutant exhibits hydrocephalus and severe cranial hemorrhage during early embryogenesis, whereas blood vessels in other regions of the embryo appear intact. Here we show that hemorrhages are associated with poor cerebral endothelial–mesenchymal contacts and an immature vascular pattern in the head. Positional cloning of bbh reveals a hypomorphic mutation in βPix, a binding partner for the p21-activated kinase (Pak) and a guanine nucleotide exchange factor for Rac and Cdc42. βPix is broadly expressed during embryonic development and is enriched in the brain and in large blood vessels. By knockdown of specific βPix splice variants, we show that they play unique roles in embryonic vascular stabilization or hydrocephalus. Finally, we show that Pak2a signaling is downstream of βPix. These data identify an essential *in vivo* role for βPix and Pak2a during embryonic development and illuminate a previously unrecognized pathway specifically involved in cerebrovascular stabilization.

angiogenesis | hemorrhage | hydrocephalus

During embryonic development, blood vessels initially form as naked endothelial tubes. In the zebrafish, the first vessels assemble and start to carry blood flow within 24 h of fertilization (1). Due to the risk of hemorrhage, stroke, and long-term neurological consequences, it is critical that nascent vessels are rapidly stabilized. Cerebral blood vessels are particularly fragile during development. In animal models, brain hemorrhage can be caused by disruption of key molecules involved in both maintaining endothelial–endothelial interactions or molecules involved in developing interactions between the endothelium and supporting cells. However, the biological processes leading to hemorrhage are not well understood.

Formation of tight associations among brain blood vessel endothelial cells is critical for regulating their integrity. Loss of cell–cell junctions between endothelial cells, by loss of the adherens junction protein β-catenin, or loss of filamin-A leads to cerebral hemorrhage, whereas animals in which endothelial tight junctions are disrupted by loss of VEZF have large permeability defects and hemorrhage (2–4).

Disruption of extracellular matrix molecules or integrin receptors also leads to vascular instability. Deletion of collagen Col4a1 or integrins α_v or β_8 leads to intracerebral hemorrhage, whereas disruption of laminin α_4 leads to peripheral hemorrhage (5–8). Whereas Col4a1 and laminin α_4 mutants display focal disruptions in endothelial basement membrane, integrin α_v or β_8 mutants have abnormal endothelial morphology and large spaces between vessels and brain parenchyma.

In the head, endothelial cells interact with smooth muscle, pericytes, astrocytes, and neuroepithelial cells, and reciprocal signaling between endothelial and support cells is critical for the recruitment of support cells to vessels. Disruption of the endothelially expressed PDGF B ligand or of PDGF receptor β results in microaneurysms from the failure of pericytes to migrate to and support blood vessels (9, 10).

p21-activated kinase (Pak)-interacting exchange factor (Pix) proteins (also known as COOL-1, p85SPR, and ARHGEF6/7) have been implicated in cytoskeletal remodeling and cell motility in cell culture systems (11–13), although their *in vivo* function remains unknown. There are two Pix genes, αPix and βPix, with multiple splice variants. Both have strong expression in the nervous system (14, 15). Here we focus on βPix. βPix binds to Pak family members, an interaction necessary for localization of Pak to the membrane, and activation by Rac or cdc42 (12, 13, 16). βPix may act downstream of cdc42 and upstream of Rac, an interaction controlled by Pak (16–18). βPix dimerization is necessary for Rac, but not cdc42, binding, suggesting a mechanism by which βPix might differentially control activation of downstream pathways (19). Although βPix is a guanine exchange factor, it also acts in a GTPase-independent mode to activate Pak through binding of GIT1, followed by localization to focal adhesions (20). βPix can also act independently of Pak by binding Cbl (21). Pix and Pak participate in multiple cellular pathways and are downstream of the EGFR, integrins, and G coupled protein receptors (19, 21, 22). The *in vivo* roles of βPix and Pak2 are unknown, but related Pix and Pak genes are critical for neural development in mice and humans (23–25).

A role for Pak in angiogenesis has been suggested from experiments in cultured endothelial cells. Dominant-negative Pak inhibits endothelial cell migration, whereas expression of a βPix-binding Pak fragment inhibits endothelial tube formation (26, 27). Pak also plays a role in permeability in human umbilical vein endothelial cells (HUVEC) and bovine aortic endothelial cells (BAEC) (28). It is not known whether βPix is required for Pak activity during angiogenesis nor whether Pak plays the same roles in angiogenesis *in vivo*.

Here we uncover previously unrecognized roles for βPix and Pak2a. Zebrafish *bubblehead* (*bbh*) mutants have a hypomorphic mutation in βPix, resulting in cerebral hemorrhage and hydro-

Author contributions: J.L., S.D.F., P.W.F., J.V.B., A.L.L., and S.J.C. designed research; J.L., S.D.F., P.W.F., E.L.R., J.V.B., O.S.-S., A.L.L., and S.J.C. performed research; J.-N.C. and F.C.S. contributed new reagents/analytic tools; J.L., S.D.F., P.W.F., J.V.B., and S.J.C. analyzed data; and J.L., S.D.F., and S.J.C. wrote the paper.

The authors declare no conflict of interest.

This article is a PNAS Direct Submission.

Abbreviations: CH, calponin homology; hpf, hours postfertilization; MO, morpholino antisense oligonucleotide; Pak, p21-activated kinase; Pix, Pak-interacting exchange factor.

Data deposition: The sequences reported in this paper have been deposited in the GenBank database [accession nos. DQ656108 (βPix-A), DQ656109 (βPix-B), and DQ656110 (Pak2a)].

§To whom correspondence should be addressed. E-mail: schilds@ucalgary.ca.

This article contains supporting information online at www.pnas.org/cgi/content/full/0700825104/DC1.

cephalus. We identify a pathway involving βPix and Pak2a in vascular stabilization during embryonic development, functions that were previously unrecognized.

Results

Loss of βPix Leads to Hemorrhage in Early Development. To identify pathways involved in developmental vascular stabilization, we took a genetic approach. *bbh*^{m292} is an *N*-ethyl-*N*-nitrosourea (ENU)-derived zebrafish mutant (29) that develops multiple cerebral hemorrhages between 36 and 52 h postfertilization (hpf). By complementation, we found a second allele, *bbh*^{fn40a}, in an independent genetic screen (30). Before the development of hemorrhages, mutants are indistinguishable from wild type and establish a robust circulation. The window of time in which hemorrhages appear corresponds to a period of active angiogenesis, when many new vessels carry flow for the first time and when hemodynamic forces are rapidly changing. Nonstereotypic, widespread hemorrhages in the head suggest a general defect in cerebral vessel stability, rather than breakage of specific vessels (Fig. 1 *A–J*). Some *bbh* mutants develop hydrocephalus, and as time progresses, blood also pools in the brain ventricles in intraventricular hemorrhages [Fig. 1 *G* and *H* and supporting information (SI) Fig. 5]. Homozygous *bbh*^{m292};Tg(flk-1:GFP) transgenic fish, double-stained for isolectin B4 (a marker of blood in zebrafish), show the close proximity of hemorrhages to large blood vessels in the head, the middle cerebral vein and the primordial midbrain and hindbrain channels, and the paired dorsal aortae (Fig. 1 *I* and *J*). Surprisingly, despite severe hemorrhage, a majority of *bbh*^{m292} homozygous embryos survive to become fertile adults, suggesting that there is a short sensitive embryonic window in which the *bbh* gene product is required for establishing blood vessel integrity.

To identify the *bbh* genetic defect, a positional cloning approach was used. We found strong linkage of *bbh*^{m292} to Z21548 between markers Z9704 and Z48722 by bulked segregant analysis. We further narrowed the interval with new markers ctg13113–2 and ctg13117–3 to a region containing the *βPix* guanine nucleotide exchange factor (Fig. 1*K*). By sequence analysis, we found a G → A transition within the splice donor site of exon 14, resulting in exclusion of exon 14 and introduction of a premature stop codon in all splice variants of the mutant protein (Fig. 1*L*). If the mutated protein were translated, it would lack the C terminus, including a dimerization domain (Fig. 1*M* and SI Fig. 6). *bbh*^{m292} is a hypomorphic mutation, because low levels of correctly spliced *βPix* mRNA remain in mutants, as detected by RT-PCR, with primers in exons 13 and 15 (Fig. 1*N*). Exon 14 is spliced into a single band in wild-type fish, whereas in *bbh*^{m292} −/− mutants, transcript missing exon 14 (lower band) is present with normally spliced transcript (upper band). In heterozygous +/− fish there is a greater proportion of normally spliced βPix over mutant βPix. We also found a linkage of *bbh*^{fn40a} to the same region of chromosome 1 (Fig. 1*K*). Extensive sequencing of βPix genomic and cDNA from *bbh*^{fn40a} mutants did not reveal any mutations in the coding region, nor were any aberrant splice variants detected. However, using quantitative PCR, we identified a significant down-regulation of βPix mRNA, suggesting that there might be a promoter or enhancer mutation in *bbh*^{fn40a} that affects βPix transcription or a mutation that affects mRNA stability (Fig. 1*O*).

To confirm that loss of *βPix* leads to hemorrhage, we designed a morpholino antisense oligonucleotide (MO) to knock down expression of βPix. *βPix*^{exon6}-MO blocks splicing of exon 6 and results in premature protein termination. Injection of 0.2 ng of *βPix*^{exon6}-MO resulted in hemorrhage in 61% of embryos (Fig. 2 *A* and *B* and SI Table 1). Higher doses of *βPix*^{exon6}-MO (up to 8 ng) result in a lack of blood circulation, and therefore no hemorrhage was detected. Injection of 8 ng of morpholino results in complete

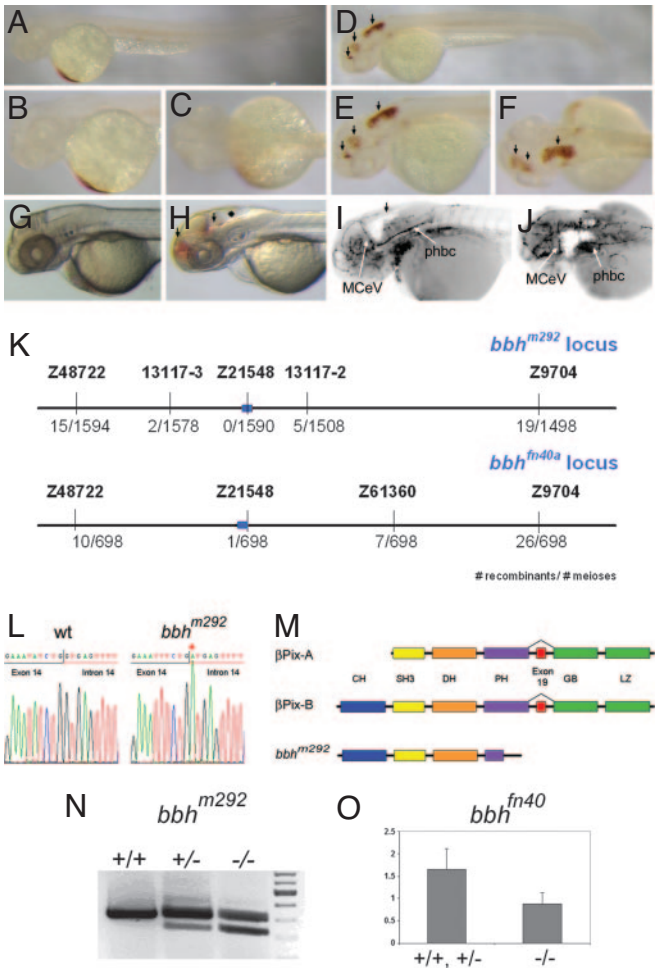

Fig. 1. *bubblehead* zebrafish develop multiple hemorrhages in the brain because of a mutation in *βPix*. (*A–F*) Isolectin staining of wild type [whole-mount (*A*), head (*B*), top view(*C*)] and *bbh*^{m292} mutant embryos with three separate hemorrhages (arrows in *D–F*). (*G* and *H*) Brain hemorrhages and hydrocephalus (*) are also visible in live mutant zebrafish. (*G*) Wild type. (*H*) *bbh*^{m292} mutant. (*I* and *J*) An overlay of isolectin staining on vascular pattern as visualized with *flk:GFP* localizes hemorrhages near the middle cerebral vein (MCeV) and primordial midbrain and hindbrain channels (PMBC and PHBC, respectively). All embryos are 52–56 hpf. (*K* and *L*) Mapping revealed linkage to chromosome 1 at the βPix locus in the *bbh*^{m292} and *bbh*^{fn40} alleles (*K*) and a splice site mutation in βPix (*L*). (*M*) Four splice variants of βPix were identified, including two variants with alternative 5′ exons and an alternatively spliced internal exon (exon 19). βPix is truncated in the pleckstrin homology domain in *bbh*^{m292} due to mutation of a splice donor site. (*N*) Amplification of βPix cDNA with primers surrounding exon 14 shows a reduction in wild type and increased mutant transcripts in *bbh*^{m292}. (*O*) *Bbh*^{fn40a} mutants have strongly reduced expression of βPix by quantitative PCR.

missplicing of *βPix* and therefore a null phenotype, whereas lower doses retain some normally spliced *βPix* (SI Fig. 7).

βPix Splice Variants Have Unique Developmental Roles. *βPix* is alternatively spliced in fish and mammals, although until now no function has been associated with different splice variants (11–15, 31). We have identified four alternatively spliced *βPix* transcripts in zebrafish (Fig. 1*M*). *βPix*-A and *βPix*-B have alternative first exons. *βPix*-B contains a previously unrecognized calponin homology (CH) domain at its N terminus, the result of transcription from a more distal promoter, whereas *βPix*-A is transcribed from a more proximal promoter. The *βPix* CH domain is highly similar to the previously reported CH

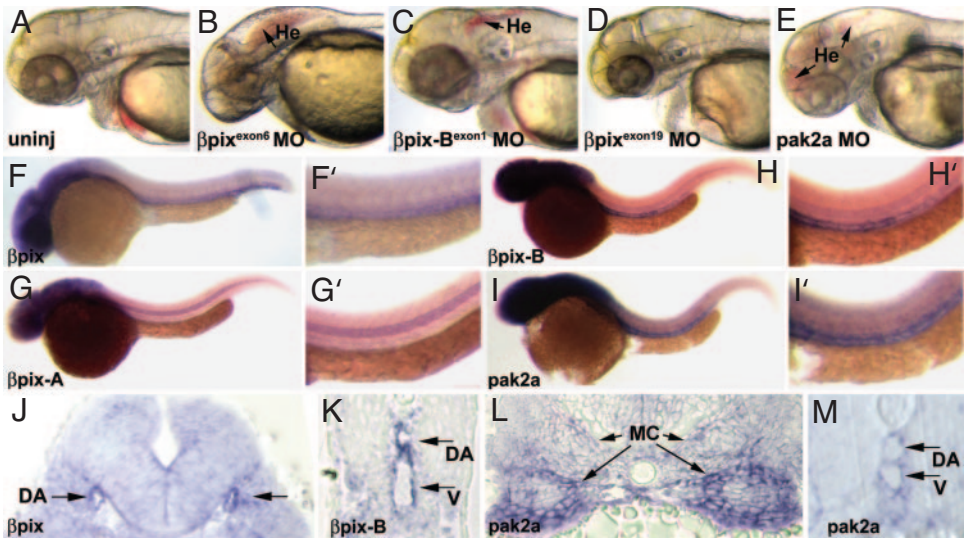

Fig. 2. βPix splice variants have unique expression and knockdown phenotypes. (*A–E*) Pan-βPix morphants, βPix-B-specific morphants, or Pak2a morphants (*A–C* and *E*) show hemorrhages in the brain with occasional hydrocephalus, whereas exon19 morphants (*D*) show hydrocephalus at high frequency at 52 hpf. (*F* and *F′*) A pan-βPix probe shows expression in the whole brain, in large blood vessels in the trunk, and the major cerebral blood vessels at 31 hpf. (*G*, *G′*, *H*, *H′*, *J*, and *K*) At 36 hpf, βPix-A and -B are expressed in the brain. Only βPix-B is expressed in the blood vessels in the trunk. (*I*, *I′*, *L*, and *M*) At 48 hpf, Pak2a is highly expressed in the mesenchymal cells around the major cerebral vessels and in the major blood vessels in the trunk. DA, dorsal aorta; V, posterior cardinal vein; He, hemorrhage; MC, mesenchymal cells.

domain of *αPix*. Although expression of *βPix*-B has not been reported in cultured cells, it is a predominant embryonic transcript. At very low levels, we detected alternative *βPix*-A and *βPix*-B variants containing exon 19. This exon corresponds to an alternatively spliced, neural-specific exon of mouse *βPix* called the "insert" region (14).

We have uncovered distinct functional roles of *βPix* splice variants during development. When the *βPix*-B splice isoform is specifically targeted using the *βPix*-B^{ATG}-MO, we observed a >50% hemorrhage rate (Fig. 2*C*), suggesting that this isoform is critical for vascular integrity. Intriguingly, when we target transcripts containing *exon 19* by using the *βPix*^{exon19}-MO, we observe >90% hydrocephalus (Fig. 2*D*) but very low levels of hemorrhage (1.1%). This observation suggests that hydrocephalus in *bbh* mutants is due to loss of *exon 19* containing transcripts and is a separable phenotype from loss of vascular integrity. Unfortunately, a morpholino targeting *βPix*-A results in high embryonic mortality. This variant cannot be studied further using morpholino technology because there is only a single morpholino design that can specifically target the short, unique *βPix*-A sequence.

To investigate the cell types involved in vascular stabilization, we determined the expression of *βPix* during development. Before 24 hpf, *βPix* is ubiquitously expressed (data not shown). At 30–36 hpf, *βPix* is most strongly expressed in the neuroepithelial cells lining the brain ventricles and in the large trunk and head blood vessels, but it also has weak ubiquitous expression (Fig. 2 *F*, *F′*, and *J*). Using probes to specific splice variants, we show that each has its own unique expression pattern. *βPix-A* is expressed highly in the brain (Fig. 2 *G* and *G′*), whereas *βPix-B* is expressed in both the brain and large blood vessels of the trunk and head (Fig. 2 *H*, *H′*, and *K*). *Exon 19* is expressed similarly to the pan-*βPix* probe but at very low levels (data not shown).

Pak2a Is a Downstream Effector of βPix. βPix was first identified as a high-affinity Pak-binding protein (11–13). We undertook an expression screen to identify Pak genes with similar expression patterns to *βPix*. We identified homologs of *Pak1*, *Pak2a*, *Pak2b*, and *Pak6*. *Pak2a* is highly expressed in the brain, in head mesenchyme around cerebral vessels, and in the dorsal aorta and posterior cardinal vein of the trunk, similar to *βPix* (Fig. 2 *I*, *I′*, and *K–M*). *Pak2b* is expressed in a similar pattern to *Pak2a*, whereas *Pak1* and *Pak6* are highly expressed in the brain (SI Fig. 8). To determine whether a knockdown of *Pak2a* phenocopies *bbh*, we targeted either the *Pak2a* translational start site (*Pak2a*^{ATG}-MO) or the exon 5 splice acceptor site (*Pak2a*^{e5i6}-MO). Injection of either morpholino results in hemorrhage, suggesting that Pak2a might function in a pathway with βPix (Fig. 2*E* and SI Table 1). Consistent with these results, Buchner *et al.*, have identified a Pak2a genetic mutant with an identical phenotype to *bbh* (D. A. Buchner, F. Su, J. S. Yamaoka, M. Kamei, J. A. Shavit, B. McGee, A. W. Hanosh, S. Kim, P. Jagadeeswaran, B. M. Weinstein, D. Ginsburg, and S. E. Lyons, unpublished data).

We undertook rescue experiments to demonstrate a genetic interaction between *βPix* and *Pak*2a in embryonic vascular integrity. Injection of a constitutively active *Pak2a*$^{T395E/\ R189G/\ P190A}$ with critical residues for binding βPix mutated (as described in ref. 13) into *bbh* homozygous mutants results in a statistically significant rescue of 17.5% ($P = 0.004$) (SI Table 2). This rescue is identical to the level of rescue when *βPix*-A RNA is injected into *bbh* mutants (17.7%, $P = 0.024$) (SI Table 3). The mutant βPix protein in *bbh*^{m292} likely acts semidominantly, because injection of *Pak2a*^{T395E}, which is constitutively active but retains sites to bind βPix, could not rescue *bbh*^{m292} (SI Table 4). Together, these knockdown and rescue experiments indicate that βPix and Pak2a function in a pathway together to stabilize blood vessels.

To determine the cell type in which βPix is required, DNA constructs expressing *βPix*-A or *βPix*-B under the endothelial-specific *flk* or *lmo2* promoters were introduced into βPix morphants. Contrary to the expected rescue, there was a significant 15–41% enhancement of hemorrhage. Because injection of *βPix*-A DNA under the β-actin promoter results in a 64% rescue of hemorrhage, this suggests that βPix function is required in a cell type other than endothelial cells (SI Tables 5–8). Incomplete rescue is likely the result of mosaic expression (SI Fig. 9).

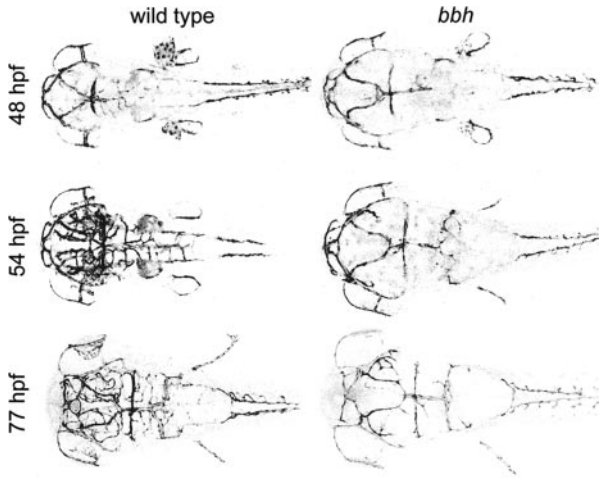

Fig. 3. Altered blood vessel pattern in *bbh*^{m292} mutants. Transgenic Flk:GFP marks developing blood vessels in wild-type and *bbh*^{m292} mutants. Although indistinguishable at 48 hpf, the extensive angiogenesis occurring between 48 and 54 hpf in wild-type embryos is lacking in mutants, with a partial recovery by 77 hpf.

Blood Vessel Function Appears Normal in *bbh*. To investigate the underlying cause of blood vessel instability and rupture, we examined whether *bbh*^{m292} mutants have gross deficiencies in clotting by an *in vitro* assay but found no significant difference as compared with wild types (SI Fig. 10). To examine potential structural defects, we stained for ZO-1 but found no gross difference in numbers of tight junctions in *bbh* (SI Fig. 11 *C*–*F*). Because βPix has been shown to interact with cdc42, a GTPase involved in vascular lumenization (13, 32), we determined whether lumenization occurred normally in *bbh* mutants and βPix morphants. We find that vessels lumenize normally in the head (SI Fig. 11 *C* and *D*) and the trunk (data not shown). Mature brain blood vessels are normally impermeable to proteins such as albumin due to the blood–brain barrier. To determine whether there were permeability defects in *bbh* mutants, we injected a fluorescent albumin derivative directly into the circulation of 2-days postfertilization (dpf) homozygous hemorrhaged fish by using angiography. Surprisingly, the dye did not localize to hemorrhages (Fig. 11 *A* and *B*), suggesting that the hemorrhage sites had clotted and vascular integrity had been reestablished after the initial catastrophic leakage of blood. Therefore, the gross function of the vasculature appears to be normal in *bbh*. We also observed that there was a slow release of labeled albumin into all tissues from the blood vessels in both mutants and wild types, suggesting that there is not a well developed blood–brain barrier in zebrafish at this developmental stage.

Vessel Pattern and Structure Is Abnormal in *bbh*. We next examined patterning and vascular ultrastructure in *bbh* mutant vessels. Because Pak promotes migration of cultured endothelial cells (26), we reasoned that vascular pattern might be affected in *bbh*. We used confocal microscopy of live *flk*:GFP transgenic fish to examine the pattern of blood vessels in developing *bbh* mutants. Mutant and wild-type vessel pattern was identical through 48 hpf, and all major blood vessels were patterned normally (Fig. 3). However, from that point on, wild-type embryos continued to develop an elaborate pattern of small cranial vessels, whereas *bbh* mutants retained an immature pattern. Thus, at 77 hpf, the *bbh*^{m292} vessel pattern is similar to that of a 48-hpf embryo.

We examined the structure of blood vessels in the head by using transmission electron microscopy (TEM). We examined up to two vessels from three 52- to 59-hpf wild-type and three

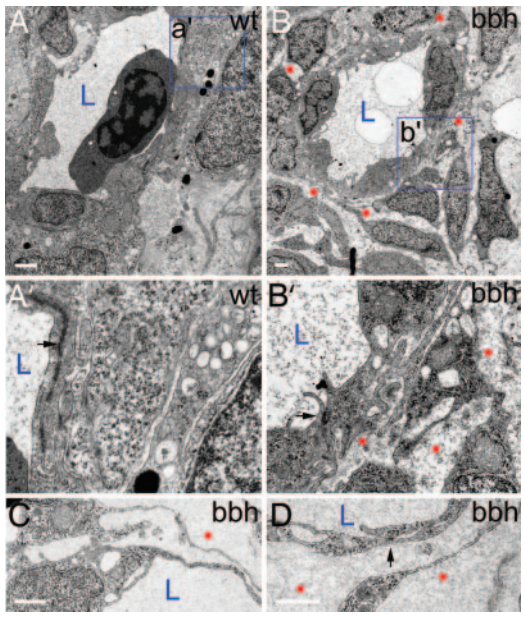

Fig. 4. Ultrastructural defects in endothelial cell–mesenchymal contacts in *bbh*^{m292} mutants. (*A* and *A*′) Normal cerebral blood vessels are closely surrounded by mesenchymal cells (*A*) and have numerous and extensive tight junctions between adjacent endothelial cells (arrow in *A*′). (*B*) In *bbh*^{m292} mutants, there is poor or no contact of endothelial cells with surrounding substratum, and *bbh*^{m292} mutant endothelial cells have a tortuous stretched abluminal surface. (*A*′ and *B*′) Enlargements of *Insets* in *A* and *B*, respectively, showing the structure of the vessel wall. (*B*, *C*′, and *D*) Endothelial cells are often stretched (*C* and *D*); however, tight junctions between the dysmorphic endothelial cells are maintained (arrows in *B*′ and *D*). L, lumen; ∗, intercellular space. (Scale bars: 1 μm.)

hemorrhaged homozygous mutant embryos. Very strikingly, clear differences in tissue structure around head vessels were seen in *bbh* mutants. Although wild-type endothelial cells are in close proximity to surrounding cells, in the most severely affected *bbh* vessels, there is essentially no contact between endothelial cells and the underlying mesenchyme. We refer to these cells as mesenchymal, because markers are not available in zebrafish to identify them as smooth muscle cells, pericytes, or astrocytes at this stage of development. The endothelial cell cytoplasm in *bbh* mutants is thin and stretched, and the vessel lumen is often larger compared with wild-type control embryos (Fig. 4). Interestingly, tight junctions are maintained between endothelial cells in *bbh*, confirming our earlier finding that endothelial cell self-contacts form normally. There was no evidence by TEM for a basement membrane on the abluminal surface of endothelial cells, reflecting the immaturity of both wild type and mutant blood vessels at this developmental stage.

Discussion

A βPix:Pak2a Pathway Stabilizes Cerebral Vasculature. We report expression of *βPix* and *Pak2a* in the embryonic vascular system and identify a role for both genes in vascular stabilization. By positional cloning we identify a hypomorphic mutation in *βPix* in *bbh*^{m292} mutants. Because βPix associates with Pak kinases, we identified a Pak with a similar expression pattern to βPix. The knockdown of *Pak2a* phenocopies the *bbh* phenotype, whereas overexpression of *Pak2a* rescues *bbh*^{m292}, suggesting that both genes act in the same genetic pathway.

It is intriguing that loss of βPix or Pak2a leads to hemorrhage in the head but not in other vascular beds. In which cell type is βPix critical for vascular stabilization? Both genes are expressed within the endothelial and peri-endothelial areas of large blood

vessels in the head and trunk. In addition, *βPix* is strongly expressed in the brain and neuroepithelial lining of the brain ventricles, whereas *Pak2a* is strongly expressed in ventral head mesenchyme. Global expression of *βPix* or *Pak2a* in *bbh* genetic mutants rescues hemorrhage, whereas expression of βPix in endothelial cells under either the *flk* or *lmo2* promoters strongly enhances vascular instability instead of rescuing. This exacerbation is consistent with βPix playing a role in support cells surrounding the cranial vasculature. Rescue experiments to define this cell type await the development of promoters for smooth muscle cells and pericytes in zebrafish.

Abnormal Cell Contacts in *bbh* Vessels. We found ultrastructural evidence of abnormal endothelial cell morphology in *bbh* vessels, with a frequent complete lack of contact between endothelium and surrounding mesenchyme. This phenotype is strikingly similar to that of mice null for integrin α_v or β_8 (33, 34), molecules which promote endothelial cell homeostasis through attachment to neuroglial cells. Pix family proteins have been implicated in cellular pathways involving integrin signaling, although the evidence is indirect. The CH domain of αPix binds to βParvin, an adaptor protein associated with integrin-linked kinase (35), a direct downstream mediator of integrin signaling. Because our report describes a previously unrecognized βPix variant with a CH domain, it is not known whether the βPix CH domain can bind to βParvin as the αPix CH domain does. βPix can also form a complex with the adaptor proteins GIT1 and paxillin, scaffolding molecules important for the localization of Pak and Rac at focal complexes where integrins are localized (36). In further support, Pak family proteins have been implicated in integrin signaling. Upon integrin $\alpha_v\beta_5$ binding to vitronectin, Pak4 becomes colocalized with this integrin (37). Therefore, reduction or loss of βPix expression might result in disruption to the paxillin/GIT/Pix/Pak complex at focal adhesions and therefore to a reduction in integrin signaling and adhesion.

βPix Is an Essential Embryonic Gene. The genetic lesion in the *βPix* gene in *bbh*^{m292} genetic mutants occurs at a splice site, preventing the splicing of exon 14 into the transcript. However, we have found that the mutation is hypomorphic, because there is both normally spliced *βPix* in *bbh*^{m292} mutants in addition to a transcript lacking exon 14. Consistent with our genetic data, low doses of morpholino (i.e., doses that would lead to a hypomorphic state) lead to hemorrhage, but higher doses of morpholino (i.e., leading to a complete null) lead to a strong cardiovascular phenotype lacking circulation and therefore lack hemorrhage. Thus, subtle alterations in *βPix* levels lead to strong developmental phenotypes. Not surprisingly, high-dose βPix morphants are nonviable, indicating an essential role for βPix during embryonic development. Hemorrhages are not necessarily lethal, because hypomorphic *bbh* mutants or βPix morphants are viable. Other genetic mutants with hemorrhage are similarly viable, for instance, the zebrafish Pak2a *redhead* mutant (D. A. Buchner, F. Su, J. S. Yamaoka, M. Kamei, J. A. Shavit, B. McGee, A. W. Hanosh, S. Kim, P. Jagadeeswaran, B. M. Weinstein, D. Ginsburg, and S. E. Lyons, unpublished data), and mouse laminin α4 mutants (8). Clotting is normal in *bbh* mutants, and a normal repair process must take place after hemorrhage.

βPix and Vascular Development. Pak has been previously implicated in endothelial cell migration, tube formation, and permeability using cultured endothelial cells (26–28). αPix, the sister gene of βPix, also regulates migration in myeloid cells (38). Therefore, we examined the role of βPix in vascular pattern (because this reflects cell migration), vessel lumenization, and permeability. We found that the initial vascular pattern is normal in *bbh* mutants and βPix morphants, and that blood vessels lumenize normally. However, we found that the pattern of vessels does not increase in complexity as it does in wild-type embryos at 72 hpf. This immaturity of vascular development could be a secondary effect of hemorrhage or could reflect a defect in migration of endothelial cells. We found we were unable to assess the role of βPix in vascular permeability because a blood–brain barrier has not yet developed in zebrafish by 48 hpf; thus, zebrafish vessels are permeable to albumin during these early stages of development. Taken together, our data suggests that βPix plays a role in vascular development that is distinct from these previously suggested roles for Pak.

Separable Roles for βPix Splice Variants. βPix splice variants have been previously described, although their biological functions have not been elucidated. Using morpholino antisense gene knockdown, we have been able to identify roles for different βPix splice variants. In *bbh* zebrafish, βPix plays a role in two developmental processes: cerebrovascular stabilization and hydrocephalus. Whereas knockdown of all βPix variants results in hemorrhage and hydrocephalus, knockdown of *βPix*-B predominantly results in hemorrhage, and knockdown of exon 19 (alternatively spliced into both *βPix*-A and *βPix*-B transcripts) predominantly results in hydrocephalus. βPix has high expression in the neuroepithelial lining of the brain ventricles, and exon 19 may be critical for specialized functions. For instance, it may directly or indirectly influence CSF secretion or be involved in ciliary function at the neuroepithelial surface.

In summary, we find a critical role for βPix and Pak2a in neurovascular development. Intraventricular hemorrhage and hydrocephalus are common complications of between 11% and 22% of preterm infants with very low birth weights and often lead to irreversible cognitive impairment (39). Nothing is known of βPix expression in human development, but it would be interesting to determine whether βPix plays a similar role in CSF homeostasis, or in stabilizing vessels in late human gestation.

Materials and Methods

Zebrafish, Primers, and Morpholinos. *bbh*^{m292}, WIK, and Tg(flk:GFP) zebrafish were maintained and staged according to standard protocols. Primer and morpholino sequences, doses, and detailed mapping information are found in *SI Methods* and SI Tables 9 and 10.

Identification of *bbh* Mutations. One hundred-eighty SSR markers were used for bulked segregation of *bbh*^{m292} and *bbh*^{fn40a}. New genetic markers ctg13117–2 and ctg13117–3 were developed on either side of *βPix*. All mapping data refers to and is consistent with the Zv2 assembly.

Full length *βPix-A* (*arhgef7b*) and *βPix-B* sequence was generated by RACE with the Marathon kit (BD Clontech, Mountain View, CA). To confirm the *bbh*^{m292} mutation, cDNA was amplified and sequenced with GEF7race 1f and GEF7race 1r, whereas genomic DNA was amplified with the primers GEF7exon12-f1 and r1.

Levels of *βPix* mRNA were determined in 3-days postfertilization (dpf) wild-type and *bbh*^{fn40a} mutant siblings by quantitative PCR and standardized against *gapdh* mRNA by using a standard Taqman reagent mixture in an ABI 7500 (Applied Biosystems, Foster City, CA). Biological replicates were amplified in triplicate, and the average Ct was determined.

***In Situ* Hybridization, Immunostaining, and Angiography.** Whole-mount *in situ* hybridization was performed as described in ref. 40. The pan-βPix probe was made from nucleotides 574-1325 of βPix-A. The βPix-A probe was made with primers βPixA^{exon1}-f and βPixA^{exon1}-r-T7. The βPix-B probe was made with primers βPix-B^{exon1}-f and βPixB^{exon1}-r-T7. Pak2a (cb422) was obtained from the

Zebrafish International Resource Center (University of Oregon, Eugene, OR). Anti ZO-1 (1/150 dilution; Zymed, South San Francisco, CA) antibody was used with methanol-acetone permeabilization and was detected with Alexafluor 555 (Molecular Probes, Eugene, OR). Blood was stained with biotinylated Isolectin B4 (Sigma, St. Louis, MO). Embryos were sectioned at 5–7 μM in JB-4 plastic medium (Polysciences, Warrington, PA). Alexafluor 555-labeled BSA (Molecular Probes) was used to assay permeability. Confocal images were made from 4–5 μM stacks.

Microscopy and Imaging. For transmission electron microscopy, embryos were fixed at 52 hpf in 2% glutaraldehyde in 0.1 M sodium cacodylate buffer (pH 7.4). Embryos were washed, postfixed with 1% osmium tetraoxide, dehydrated, stained with 2% uranyl acetate, dehydrated to 100% ethanol, washed in propylene oxide, and embedded. Eighty nanometer sections were cut and stained with 3% uranyl acetate and Reynolds lead citrate.

Morpholino and Rescue Experiments. Full-length βPix-A or βPix-B was cloned by using the primers βPixA^{EcoRI} (or βPixB ^{EcoRI}) and βPix HA. Full-length *Pak2a* (DQ656110) was cloned with Pak2-myc and Pak2–3′. A non-βPix binding *Pak2a* was constructed using the mutagenic primers Pak2$^{RP\text{-}GA}$-f and Pak2$^{RP\text{-}GA}$-r, inducing R193G and P194A mutations. Constitutively active *Pak2a*^{T395E} was constructed with the mutagenic primers Pak2-CA-f and Pak2-CA-r. A triple mutant was made by repeating the RP-GA mutagenesis on *Pak2a*^{T395E}. Hemorrhage was scored at 52 hpf.

We thank Leona Barclay (Microscopy and Imaging Facility, University of Calgary) for electron microscopy, and Joanne Chan, Sarah McFarlane, and Ryan Lamont for helpful comments. S.D.F. was funded by a Strategic Training Program Fellowship in Genetics, Child Development, and Health from the Canadian Institutes of Health Research. S.J.C. is a Scholar of the Alberta Heritage Foundation for Medical Research and of the Heart and Stroke Foundation of Canada and holds a Tier II Canada Research Chair. Operating funds are from the March of Dimes Birth Defects Foundation and the Heart and Stroke Foundation of Alberta, Nunavut, and Northwest Territories.

1. Isogai S, Horiguchi M, Weinstein BM (2001) *Dev Biol* 230:278–301.
2. Cattelino A, Liebner S, Gallini R, Zanetti A, Balconi G, Corsi A, Bianco P, Wolburg H, Moore R, Oreda B, *et al.* (2003) *J Cell Biol* 162:1111–1122.
3. Feng Y, Chen MH, Moskowitz IP, Mendonza AM, Vidali L, Nakamura F, Kwiatkowski DJ, Walsh CA (2006) *Proc Natl Acad Sci USA* 103:19836–19841.
4. Kuhnert F, Campagnolo L, Xiong JW, Lemons D, Fitch MJ, Zou Z, Kiosses WB, Gardner H, Stuhlmann H (2005) *Dev Biol* 283:140–156.
5. Gould DB, Phalan FC, Breedveld GJ, van Mil SE, Smith RS, Schimenti JC, Aguglia U, van der Knaap MS, Heutink P, John SW (2005) *Science* 308:1167–1171.
6. McCarty JH, Monahan-Earley RA, Brown LF, Keller M, Gerhardt H, Rubin K, Shani M, Dvorak HF, Wolburg H, Bader BL, *et al.* (2002) *Mol Cell Biol* 22:7667–7677.
7. Zhu J, Motejlek K, Wang D, Zang K, Schmidt A, Reichardt LF (2002) *Development (Cambridge, UK)* 129:2891–2903.
8. Thyboll J, Kortesmaa J, Cao R, Soininen R, Wang L, Iivanainen A, Sorokin L, Risling M, Cao Y, Tryggvason K (2002) *Mol Cell Biol* 22:1194–1202.
9. Leveen P, Pekny M, Gebre-Medhin S, Swolin B, Larsson E, Betsholtz C (1994) *Genes Dev* 8:1875–1887.
10. Soriano P (1994) *Genes Dev* 8:1888–1896.
11. Oh WK, Yoo JC, Jo D, Song YH, Kim MG, Park D (1997) *Biochem Biophys Res Commun* 235:794–798.
12. Bagrodia S, Taylor SJ, Jordon KA, Van Aelst L, Cerione RA (1998) *J Biol Chem* 273:23633–23636.
13. Manser E, Loo TH, Koh CG, Zhao ZS, Chen XQ, Tan L, Tan I, Leung T, Lim L (1998) *Mol Cell* 1:183–192.
14. Kim S, Kim T, Lee D, Park SH, Kim H, Park D (2000) *Biochem Biophys Res Commun* 272:721–725.
15. Kim T, Park D (2001) *Mol Cells* 11:89–94.
16. Obermeier A, Ahmed S, Manser E, Yen SC, Hall C, Lim L (1998) *EMBO J* 17:4328–4339.
17. Cau J, Hall A (2005) *J Cell Sci* 118:2579–2587.
18. ten Klooster JP, Jaffer ZM, Chernoff J, Hordijk PL (2006) *J Cell Biol* 172:759–769.
19. Feng Q, Baird D, Cerione RA (2004) *EMBO J* 12:12.
20. Loo TH, Ng YW, Lim L, Manser E (2004) *Mol Cell Biol* 24:3849–3859.
21. Feng Q, Baird D, Peng X, Wang J, Ly T, Guan JL, Cerione RA (2006) *Nat Cell Biol* 8:945–956.
22. Bagrodia S, Cerione RA (1999) *Trends Cell Biol* 9:350–355.
23. Qu J, Li X, Novitch BG, Zheng Y, Kohn M, Xie JM, Kozinn S, Bronson R, Beg AA, Minden A (2003) *Mol Cell Biol* 23:7122–7133.
24. Kutsche K, Yntema H, Brandt A, Jantke I, Nothwang HG, Orth U, Boavida MG, David D, Chelly J, Fryns JP, *et al.* (2000) *Nat Genet* 26:247–250.
25. Allen KM, Gleeson JG, Bagrodia S, Partington MW, MacMillan JC, Cerione RA, Mulley JC, Walsh CA (1998) *Nat Genet* 20:25–30.
26. Kiosses WB, Daniels RH, Otey C, Bokoch GM, Schwartz MA (1999) *J Cell Biol* 147:831–844.
27. Kiosses WB, Hood J, Yang S, Gerritsen ME, Cheresh DA, Alderson N, Schwartz MA (2002) *Circ Res* 90:697–702.
28. Stockton RA, Schaefer E, Schwartz MA (2004) *J Biol Chem* 279:46621–46630.
29. Stainier DY, Fouquet B, Chen JN, Warren KS, Weinstein BM, Meiler SE, Mohideen MA, Neuhauss SC, Solnica-Krezel L, Schier AF, *et al.* (1996) *Development (Cambridge, UK)* 123:285–292.
30. Chen J-N, van Bebber F, Goldstein AM, Serluca FC, Jackson D, Childs S, Serbedzija GN, Warren KS, Mably JD, Lindahl P, *et al.* (2001) *Comp Funct Genom* 2:60–68.
31. Rhee S, Yang SJ, Lee SJ, Park D (2004) *Biochem Biophys Res Commun* 318:415–421.
32. Bayless KJ, Davis GE (2002) *J Cell Sci* 115:1123–1136.
33. McCarty JH, Lacy-Hulbert A, Charest A, Bronson RT, Crowley D, Housman D, Savill J, Roes J, Hynes RO (2005) *Development (Cambridge, UK)* 132:165–176.
34. Proctor JM, Zang K, Wang D, Wang R, Reichardt LF (2005) *J Neurosci* 25:9940–9948.
35. Rosenberger G, Jantke I, Gal A, Kutsche K (2003) *Hum Mol Genet* 12:155–167.
36. Zhao ZS, Manser E, Loo TH, Lim L (2000) *Mol Cell Biol* 20:6354–6363.
37. Zhang H, Li Z, Viklund EK, Stromblad S (2002) *J Cell Biol* 158:1287–1297.
38. Li Z, Hannigan M, Mo Z, Liu B, Lu W, Wu Y, Smrcka AV, Wu G, Li L, Liu M, *et al.* (2003) *Cell* 114:215–227.
39. Kazan S, Gura A, Ucar T, Korkmaz E, Ongun H, Akyuz M (2005) *Surg Neurol* 64 Suppl 2:S77–81.
40. Jowett T, Lettice L (1994) *Trends Genet* 10:73–74.